Supporting Information

On the origin of the surface superhydrophobicity of rough-textured inorganic materials with intrinsic hydrophilicity

Ruihang Wen, ‡[a] Xiaobing Chen, ‡ [a] Gaocan Qi,*[a] Wenbin Li, [a] Zhihao Yuan*[a]

[a]School of Materials Science and Engineering, Tianjin Key Lab of Photoelectric Materials & Devices, and Key Laboratory of Display Materials and Photoelectric Devices (Ministry of Education)

Tianjin University of Technology

Tianjin 300384, P. R. China

*E-mail: gaocanqi@tjut.edu.cn *E-mail: zhyuan@tjut.edu.cn

‡ These authors contributed equally to this work.

Table of Contents

Experimental section

All reagents used were of analytical grade or better. Inorganic compounds were prepared via previously reported solution approaches but with changed synthesis parameters.

Synthesis of oriented hexagonal ZnS nanorods

4.50 mmol $(NH_2)_2CS$ were dissolved into 30 ml $N_2H_4 \cdot H_2O$. A piece of Zn flake with dimensions 20 mm × 40 mm ×1 mm size was smoothed with sandpaper first, and then ultrasonically washed in de-ionized water and absolute ethanol for 10 min. After that, the Zn flakes and the growth solution were combined and placed into the Teflon autoclave, and maintained at 140 °C for 6 h. After cooling to room temperature, the Zn flake was taken out from the solution and washed several times with de-ionized water and ethanol, and then dried in a blast drying oven.

Synthesis of CuS microrod film

The CuS microrod film was synthesized by the hydrothermal method reported in the literature.[1] 1.0 mmol $Cu(NO_3)_2 \cdot 3H_2O$ and 2.0 mmol NH_4F were dissolved in 24 mL distilled water, and the solution was stirred at room temperature for 15 min. Then, 6.0 mmol $(NH_2)_2CS$ was added in the above solution with stirring. The mixed solution was transferred into a Teflon-lined autoclave of 30 mL capacity. After being sealed and heated at 120 °C for 6 h, the autoclave was cooled to room temperature naturally. The resulting black products were collected by filtration, washed with distilled water and ethanol for several times, and finally dried in air at 70 °C for 6 h. The obtained CuS powder was dispersed in ethanol and then coated on a glass slide. The CuS microrod film was obtained after drying the sample at 60 °C for 12 h.

Synthesis of Ni₃S₂ nanoplates

4.5 mmol $(NH_2)_2CS$ were dissolved into 30 ml $N_2H_4 \cdot H_2O$ with stirring. A piece of Ni foam with dimensions 20 mm × 40 mm size was ultrasonically washed in de-ionized water and absolute ethanol for 10 min. After that, the Ni foam and the growth solution were combined and placed into the Teflon autoclave, and maintained at 140 °C for 6 h. After cooling to room temperature, the Ni foam was taken out from the solution and washed several times with de-ionized water and ethanol, and then dried in a blast drying oven.

Synthesis of PbSe microparticle film

In the first step, a 0.2 mol/L Na_2Se_3 solution was prepared by dissolving 25.2g $Na_2SO_3 \cdot 7H_2O$ in 200 ml DI water. Then, 3.2 g Se powder was added, and the mixture was refluxed at 90 °C for 24 h. After refluxing, the solution was filtered to obtain a clear solution, which was then stored in the dark in a brown reagent bottle. Next, PbSe microparticles were prepared. First, 10 mL 0.2 mol/L $Pb(CH_3COO)_2$ solution was mixed with 10 mL 1.0 mol/L Trisodium citrate in 60 mL DI water. When the mixture was homogeneous, 10 mL of 1.0 mol/L KOH was added, followed by the slow addition of 10 mL of 0.2 mol/L Na_2Se_3 to form a black precipitate. The product was then centrifuged, washed several times with deionized water, absolute ethanol, and acetone, and finally dried naturally. The PbSe microparticle film was prepared using a coating method similar to that of the CuS microrod film.

Synthesis of CaF_2 film

Calcium fluoride (CaF_2) was prepared by a simple liquid-phase method. Stoichiometric calcium carbonate ($CaCO_3$) and hydrofluoric acid (HF) were mixed in a plastic bottle. After reacting for 10 h with stirring, the CaF_2 precipitate was filtered and then washed with DI water until neutral. The CaF_2 film was prepared using the coating method similar to that of CuS.

Synthesis of AgCl nanoparticle film

Starting aqueous solutions of $AgNO_3$ (4mM) and NaCl (4mM) were first prepared. 50 ml $AgNO_3$ solution was placed on a magnetic stirrer, and then a peristaltic pump was used to inject 50 ml NaCl solution into the above solution at a speed of 10 mL/min. After the reaction was completed, the solution was stirred continuously until it became clear, allowing the precipitate to settle to the bottom. The AgCl precipitate was rinsed several times with de-ionized water. The entire experimental process had to be carried out in a dark room. The AgCl nanoparticle film was prepared using a coating method similar to that of the CuS.

Synthesis of AgBr microparticle film and AgI microcluster film

AgBr microparticle film and AgI microcluster film were prepared in the same manner as AgCl nanoparticle film, except that NaCl (4 mM) were replaced by NaBr (4 mM) and KI (4 mM), respectively.

Characterization analysis

The morphology of as-prepared samples was characterized by field-emission scanning electron microscopy (FE-SEM, JEOL JSM-6700). X-ray photoelectron spectroscopies (XPS) of oriented hexagonal ZnS nanorods film and AgCl nanoparticle powder dried in air were performed on XPS. ESCA Thermo Fischer Scientific Multilab 2000 using monochromatic Al Kα radiation.

Raman scattering spectra of oriented hexagonal ZnS nanorods film and AgCl nanoparticle film were recorded with high resolution laser confocal Micro Raman spectrometer (HORIBA EVOLUTION), using a 532 nm laser beam.

The wetting properties of as-prepared samples were characterized by measuring the contact angle of 3μL water-droplet using a drop shape analysis system (DSA 100, Krüss Germany).

Quantification of H_2O_2 Production

To ensure temperature and humidity control during H_2O_2 production, we conducted the condensation experiment in a temperature-humidity test chamber, setting the temperature to 25°C and the humidity to 55%. In the cooling step, we maintained a temperature of 3 °C using a cooling station (TC40, Krüss, Germany), which resulted in condensing microdroplets with diameters ranging from 5 to 10 μm. The condensing times for ZnS and AgCl samples were set to 90 seconds and 100 seconds, respectively.

The concentration of H_2O_2 in the droplets was determined by PTO and spectrophotometry with a detection wavelength of 400 nm, referred to previously reported detection methods.[2]A 0.1 M PTO ($C_4K_2O_9Ti·2H_2O$; AR; aladdin) solution was prepared. To develop the calibration curve, 200 μL of a H_2O_2 standard solution with concentration of 0, 10, 25, 50 and 100 μM/L was added into 200 μL of PTO solution. Its absorbance at 400 nm was measured using a UV-vis spectra (Lambda U-3900). An identical procedure was conducted on microdroplet samples where 200 μL of collected microdroplets was combined with PTO. The H_2O_2 concentration of microdroplet samples could be determined from the calibration curve.

DFT calculations

All density functional theory (DFT) calculations were carried out using the Dmol^3 code. Spin-unrestricted DFT within the generalized-gradient approximation (GGA) in the form of Perdew-Burke-Emzerhof (PBE) functional was used for the calculation. In addition, the effective core potential (ECP) and a double numerical basis set including d polarization function (DNP) were used to obtain all the results. Slab model with 8 layers and p (3×2) supercell for ideal ZnS-(10$\bar{1}$0) surfaces was cut from the bulk wurtzite structure. Ideal AgCl-(100) surface was cut from the bulk rocksalt structure with 6 layers and p (3×2) supercell. Defective crystal surfaces with V_a defects were constructed by removing a sulfur atom or a chlorine atom at the top atomic layer from the ideal surfaces. A vacuum region with thickness of 15 Å was added on the slabs to separate the surface from its periodic image, and the bottom two layers were fixed while the other layers were relaxed during the optimization of all structures. For adsorption calculations, the Brillouin zone was sampled by 6×4×1 k points and the real-space orbital cutoff radius was set to be 6 Å. O_2^{2-}, O_2^-, O_2, N_2 and H_2O were chosen as the adsorbates. The calculation for O_2^{2-} and O_2^- are realized by setting their charge options to -2 and -1, respectively, in the Dmol^3 package, and by changing the charge of each oxygen atom to -1 and -1/2. A number of adsorption sites on the ideal and defective ZnS and AgCl crystal facets were examined to locate the lowest-energy configuration for the adsorption system. The adsorption energy of gas molecules on crystal surfaces, E_{ad}, was calculated as $E_{ad} = E_{total[adsorbate\ on\ crystal\ plane]} - E_{total[crystal\ plane]} - E_{total[adsorbate]}$, where E_{total} is the total energy of the system. Hence, a "-" sign in the calculation results means an exothermic process.

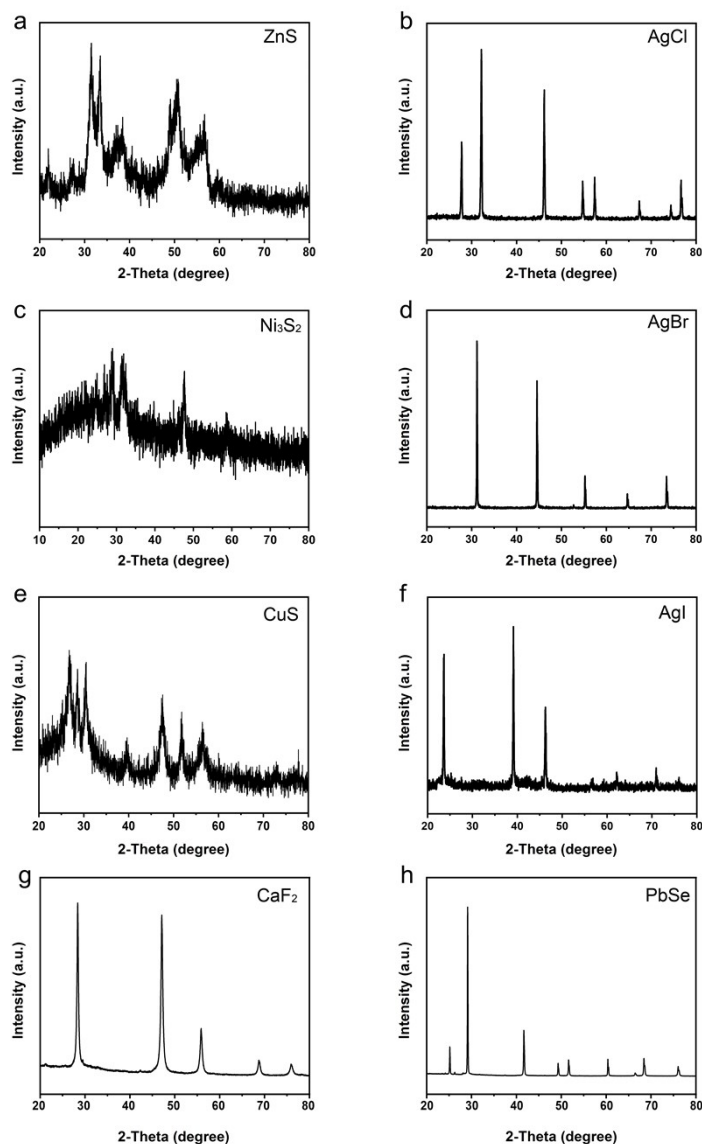# 1. XRD patterns of as-prepared inorganic compounds.

Figure S1. XRD patterns of as-prepared inorganic compounds. (a) oriented hexagonal ZnS nanorods; wurtzite phase (JCPDS No. 79-2204). (b) AgCl nanoparticles; rocksalt phase (JCPDS No 06-0480). (c) Ni_3S_2 nanoplates, heazlewoodite phase (JCPDS No.85-0775) (d) AgBr microparticles, bromargyrite phase (JCPDS No 01-0950) (e) CuS microrods, covelite phase (JCPDS No.06-0464) (f) AgI microclusters, Iodargyrite phase (JCPDS No 78-0641) (g) CaF_2 microparticles, Fluorite phase (JCPDS No 35-0816) (h) PbSe microparticles, clausthalite phase (JCPDS No 06-0354).

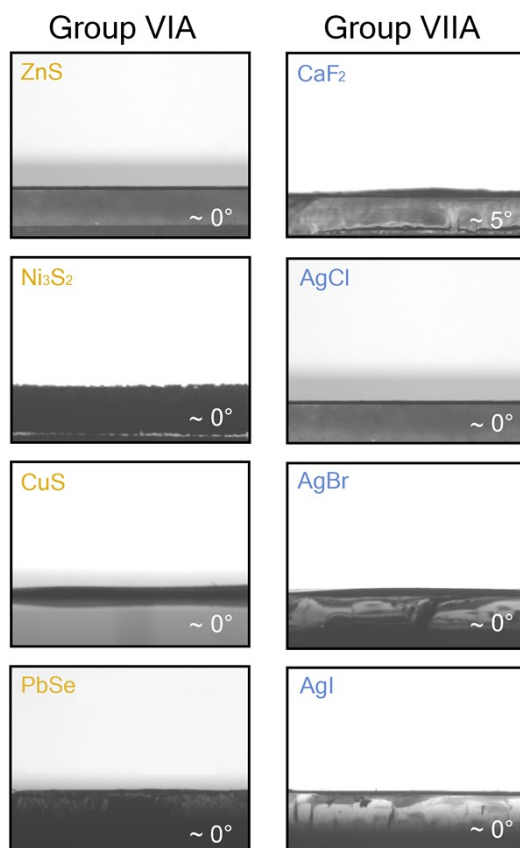**2. The water contact angles of the fresh prepared inorganic materials.**

Group VIA   Group VIIA

ZnS   CaF$_2$
~ 0°   ~ 5°

Ni$_3$S$_2$ AgCl
~ 0°   ~ 0°

CuS   AgBr
~ 0°   ~ 0°

PbSe   AgI
~ 0°   ~ 0°

Figure S2. The water contact angles of freshly prepared metal compounds of Group VIA and Group VIIA, which were dried in air.

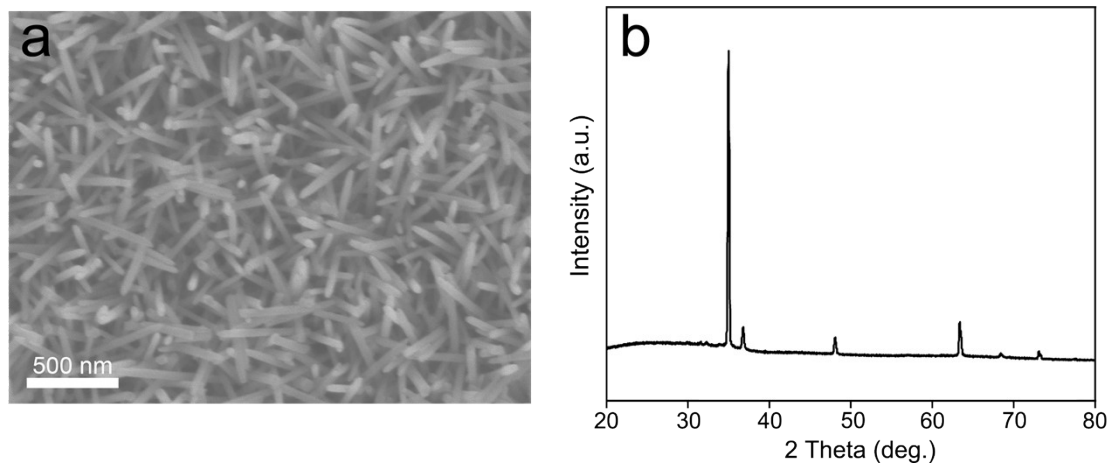## 3. The SEM image and XRD pattern of ZnO nanowires.

Figure S3. Topographic structure (a) and XRD pattern (b) of ZnO nanowires, wurtzite phase (JCPDS No. 36-1451).

4. UV-visible spectra and calibration curve of hydrogen peroxide mixed with a PTO ($K_2TiO(C_2O_4)_2 \cdot H_2O$) solution.
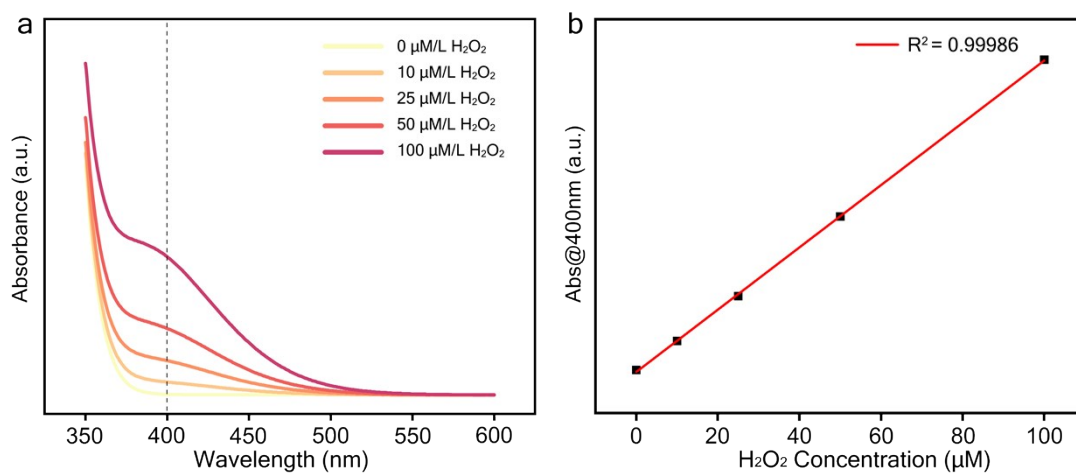

Figure S4. (a) The absorption spectrum of aqueous PTO solution with added H_2O_2. (b) Calibration curve of the absorption at 400 nm acquired from spectra shown in a.

5. The most stable adsorption configurations for O$_2$, O$_2^-$, O$_2^{2-}$ on Va sites of the Vs-ZnS (10$\bar{1}$0), V$_{Cl}$-AgCl (100) and Vo-ZnO (10$\bar{1}$0) planes, respectively.
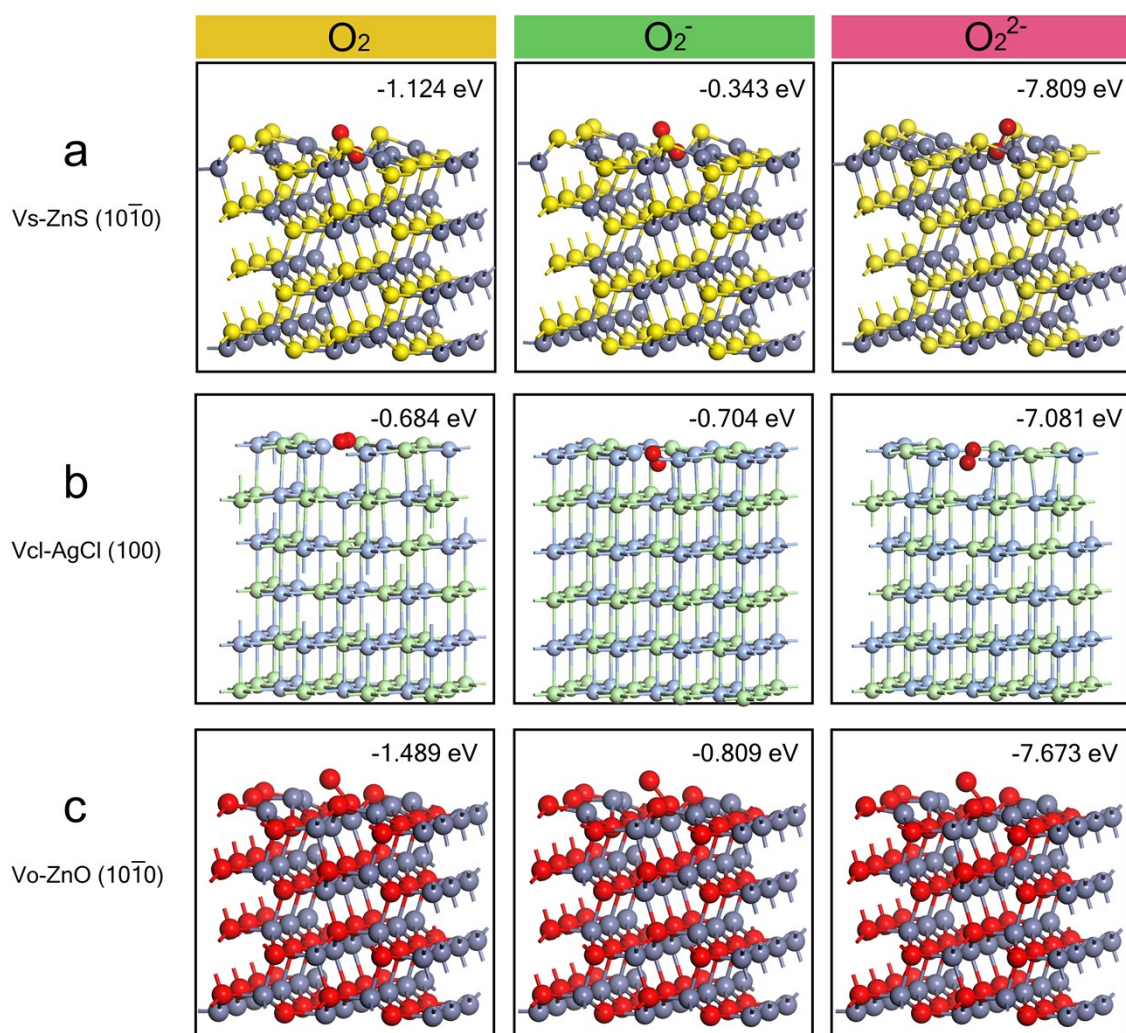

Figure S5. The most stable configurations and adsorption energies for O$_2$, O$_2^-$ and O$_2^{2-}$ on the defective planes with vacancy concentration of 1/6 monolayer. (a) Vs-ZnS (10$\bar{1}$0). (b) V$_{Cl}$-AgCl (100). (c) Vo-ZnO (10$\bar{1}$0). The red, yellow, gray, green and cyan spheres denote O, S, Zn, Cl and Ag atoms, respectively.

6. The adsorption energy for O$_2$ and O$_2^-$ on the O$_2^{2-}$-adsorbed Vo sites of Vo-ZnO (10$\bar{1}$0) plane.
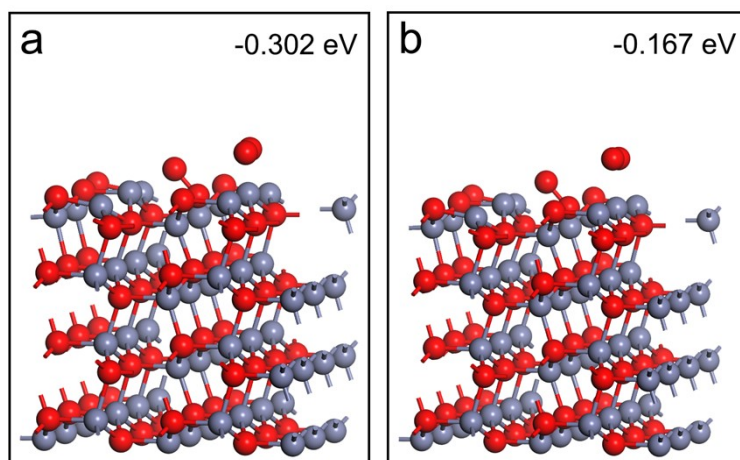

Figure S6. (a) The adsorption energy for O$_2$ on the O$_2^{2-}$-adsorbed Vo site of Vo-ZnO (10$\bar{1}$0) plane. (b) The adsorption energy for O$_2^-$ on the O$_2^{2-}$-adsorbed Vo site of Vo-ZnO (10$\bar{1}$0) plane.

7. The S 2p XPS spectra and the water contact angles of ZnS samples with varying sulfur vacancy content.
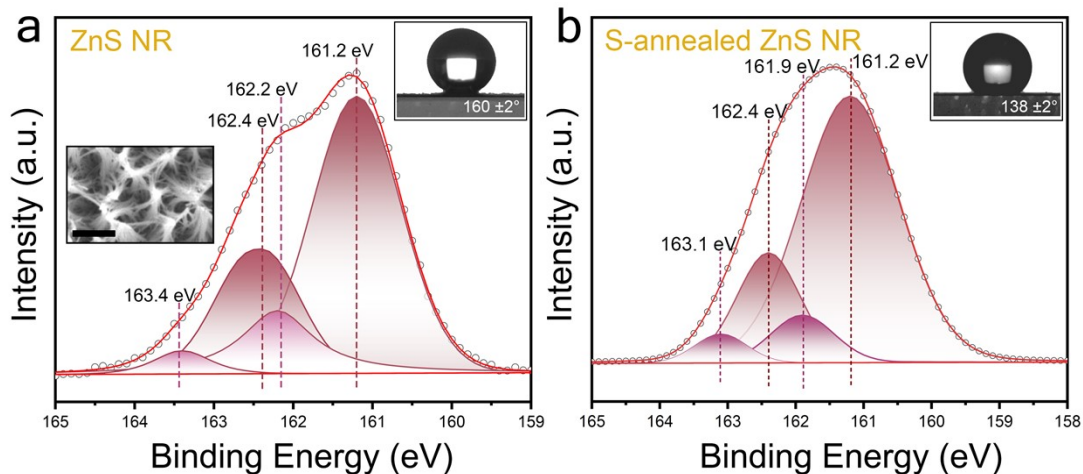

Figure S7. (a) S 2p XPS spectra of as-prepared ZnS nanorods (NR). (b) S 2p XPS spectra of the ZnS sample annealed at 420°C for 1 h in sulfur atmosphere. The insets in the top-right of S7a and S7b show the water contact angles on the corresponding samples. The right inset of S7a displays the SEM image of ZnS nanorods. scale bars: 5 μm.

As discussed in the manuscript, the binding energies at 162.2 eV and 163.4 eV are considered to originate from S atoms in the vicinity. Figure S7b shows that the S vacancy content is reduced when the sample is annealed in sulfur atmosphere.

Table S1. Surface energies of typical ZnS, Ni$_3$S$_2$, CuS, CaF$_2$, and PbSe crystal planes.

Crystal plane	Surface energy (mJ/m^2)
ZnS-(110)	650[3]
Ni$_3$S$_2$-(100)	2200[4]
CuS-(001)	1800[5]
CaF$_2$-(110)	723[6]
PbSe-(111)	1585[7]
H$_2$O (Equilibrium conditions)	~ 72[8]

The surface energies of these inorganic materials are significantly greater than the surface energy of water.

Reference

(1) Q.-L. Huang, H. Chen, Y. C. Zhang and C. Le Wu, CuS nanostructures prepared by a hydrothermal method, Journal of Alloys and Compounds, 2011, **509**, 6382-6387.

(2) Lee, J. K.; Walker, K. L.; Han, H. S.; Kang, J.; Prinz, F. B.; Waymouth, R. M.; Nam, H. G.; Zare, R. N. Spontaneous generation of hydrogen peroxide from aqueous microdroplets. *Proceedings of the National Academy of Sciences of the United States of America* 2019, *116*, 19294-19298.

(3) Wright, K.; Watson, G. W.; Parker, S. C.; Vaughan, D. J. Simulation of the structure and stability of sphalerite (ZnS) surfaces. *American Mineralogist* 1998, *83*, 141-146.

(4) Zhang, B.; Fu, X.; Song, L.; Wu, X. Surface selectivity of Ni_3S_2 toward hydrogen evolution reaction: a first-principles study. *Physical Chemistry Chemical Physics* 2020, *22*, 25685-25694.

(5) Soares Jr., A. L.; Dos Santos, E. C.; Morales-García, Á.; Duarte, H. A.; De Abreu, H. A. The stability and structural, electronic and topological properties of covellite (001) surfaces. *ChemistrySelect* 2016, *1*, 2730-2741.

(6) Janicki, M. J.; Drzymala, J.; Kowalczuk, P. B. Structure and surface energy of both fluorite halves after cleaving along selected crystallographic planes. *Physicochemical Problems of Mineral Processing* 2016, *52*, 451-458.

(7) Deringer, V. L.; Dronskowski, R. Stabilities and reconstructions of clean pbs and pbse surfaces: DFT results and the role of dispersion forces. *The Journal of Physical Chemistry C* 2016, *120*, 8813-8820.

(8) Hauner, I. M.; Deblais, A.; Beattie, J. K.; Kellay, H.; Bonn, D. The Dynamic Surface Tension of Water. The Journal of Physical Chemistry Letters 2017, **8**, 1599-1603.